ELSEVIER

Journal of Organometallic Chemistry 505 (1995) 1–9

Journal of Organometallic Chemistry

Ligand substitution of the redox-active diphosphine 4,5-bis(diphenylphosphino)-4-cyclopenten-1,3-dione (bpcd) in the alkynyl-bridged cluster $Ru_3(CO)_9(\mu_2\text{-}H)(\mu_3\text{-}\eta^2\text{-}C{\equiv}C^tBu)$. Synthesis, X-ray structure and electrochemical properties of $Ru_3(CO)_7(\mu_2\text{-}H)(\mu_3\text{-}\eta^2\text{-}C{\equiv}C^tBu)$(bpcd)

Huafeng Shen, Travis J. Williams, Simon G. Bott *, Michael G. Richmond *

Department of Chemistry, Center for Organometallic Research and Education, University of North Texas, Denton, TX 76203, USA

Received 10 January 1995; in revised form 22 March 1995

Abstract

The alkynyl-bridged triruthenium cluster $Ru_3(CO)_9(\mu_2\text{-}H)(\mu_3\text{-}\eta^2\text{-}C{\equiv}C^tBu)$ (**1**) reacts with the redox-active diphosphine ligand 4,5-bis(diphenylphosphino)-4-cyclopenten-1,3-dione (bpcd) in the presence of Me_3NO to afford the new cluster $Ru_3(CO)_7(\mu_2\text{-}H)(\mu_3\text{-}\eta^2\text{-}C{\equiv}C^tBu)$(bpcd) (**2**) in 76% yield. The diphosphine ligand in **2** is bound at the unique ruthenium atom in a chelating fashion, and is the first example of a cluster-coordinated bpcd ligand. Cluster **2** has been characterized in solution by IR and NMR (^1H and ^{31}P) spectroscopy and in the solid state by X-ray diffraction analysis. $Ru_3(CO)_7(\mu_2\text{-}H)(\mu_3\text{-}\eta^2\text{-}C{\equiv}C^tBu)$(bpcd), as the CH_2Cl_2 solvate, crystallizes in the monoclinic space group $P2_1/c$: $a = 21.190(1)$ Å, $b = 12.345(1)$ Å, $c = 17.272(1)$ Å, $\beta = 95.075(5)°$, $V = 4500.5(5)$ Å^3, $Z = 4$, $d_{calc} = 1.667$ g cm^{-3}; $R = 0.0399$, $R_w = 0.0432$ for 3255 observed reflections. The redox properties of **2** were explored by cyclic voltammetry, which revealed the presence of a reversible one-electron reduction process (bpcd based) and an irreversible oxidation (metal based). The nature of the HOMO and LUMO in **2** has been examined by carrying out extended Hückel MO calculations on the model cluster $Ru_3(CO)_7(\mu_2\text{-}H)(\mu_3\text{-}\eta^2\text{-}C{\equiv}CH)(H_4\text{-bpcd})$, and the results are discussed with respect to the observed electrochemistry. The propensity of cluster **2** to undergo P–C bond cleavage is discussed in the light of other diphosphine ligand work.

Keywords: Ruthenium; Metal clusters; Alkynes; Phosphines; Oxidative addition

1. Introduction

The reaction between $Ru_3(CO)_{12}$ and alkynes has been extensively studied over the last few years with regard to cluster-assisted activation of the alkyne ligand [1]. For the reaction between the terminal alkyne 3,3-dimethylbut-1-yne and $Ru_3(CO)_{12}$, the cluster $Ru_3(CO)_9(\mu_2\text{-}H)(\mu_3\text{-}\eta^2\text{-}C{\equiv}C^tBu)$ (**1**) may be isolated in high yields by carefully monitoring the thermolysis reaction [2]. This cluster is of interest because it contains a bridging hydride ligand, as a result of an alkyne C–H bond activation, and a 5e$^-$ donor $\mu_3\text{-}\eta^2$-alkyne moiety. The structural composition of this cluster and others of its genre has been fully characterized by X-ray and neutron diffraction techniques [2–4].

The triruthenium cluster $Ru_3(CO)_9(\mu_2\text{-}H)(\mu_3\text{-}\eta^2\text{-}C{\equiv}C^tBu)$ exhibits rich reaction chemistry. It has been employed as a starting material in the construction of mixed-metal clusters [5] and has been shown to react with phosphine ligands in a manner that is dependent on the nature of phosphine. Monodentate phosphine ligands undergo regiospecific substitution at an equatorial site on the unique ruthenium atom to give $Ru_3(CO)_8(\mu_2\text{-}H)(\mu_3\text{-}\eta^2\text{-}C{\equiv}C^tBu)(PR_3)$, as demonstrated by X-ray diffraction analysis; however, solution NMR measurements have revealed the existence of a tripodal rotation process that serves to equilibrate the phosphine ligand about the equatorial and axial positions [6].

* Corresponding authors.

SSDI 0022-328X(95)05564-9

Bidentate phosphine ligands react with $Ru_3(CO)_9(\mu_2\text{-}H)(\mu_3\text{-}\eta^2\text{-}C{\equiv}C^tBu)$ to give both chelating and bridging isomers of $Ru_3(CO)_7(\mu_2\text{-}H)(\mu_3\text{-}\eta^2\text{-}C{\equiv}C^tBu)(P\text{–}P)$ depending on the nature of the diphosphine ligand. For example, whereas the rigid ligands dppm and (*Z*)-$Ph_2PCH{=}CHPPh_2$ give only single products arising from bridging of a hydride-free edge and chelating of the unique ruthenium center, respectively, the flexible diphosphine ligand dppe gives a mixture of bridging and chelating isomers [7].

We have recently begun a program designed to study the interactions between redox-active diphosphine ligands and polynuclear cluster compounds [8]. Accordingly, we were interested in examining the substitution chemistry of $Ru_3(CO)_9(\mu_2\text{-}H)(\mu_3\text{-}\eta^2\text{-}C{\equiv}C^tBu)$ with the redox-active diphosphine ligand 4,5-bis(diphenylphosphino)-4-cyclopenten-1,3-dione (bpcd).

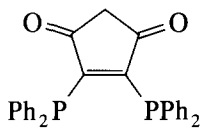

bpcd

Our interest in this particular diphosphine ligand stems from a lack of organometallic compounds that are substituted by this ligand [9], coupled with our observation of facile P–C bond cleavage exhibited by the bpcd ligand in other polynuclear cluster complexes [10], behavior that we hoped would be observed in $Ru_3(CO)_7(\mu_2\text{-}H)(\mu_3\text{-}\eta^2\text{-}C{\equiv}C^tBu)$(bpcd). Herein we report our data on the synthesis, X-ray diffraction structure and electrochemistry of $Ru_3(CO)_7(\mu_2\text{-}H)(\mu_3\text{-}\eta^2\text{-}C{\equiv}C^tBu)$(bpcd). Extended Hückel MO calculations were performed on the model cluster compound $Ru_3(CO)_7(\mu_2\text{-}H)(\mu_3\text{-}\eta^2\text{-}C{\equiv}CH)(H_4\text{-bpcd})$, the results being compared with the redox data obtained from $Ru_3(CO)_7(\mu_2\text{-}H)(\mu_3\text{-}\eta^2\text{-}C{\equiv}C^tBu)$(bpcd).

2. Results and discussion

2.1. Synthesis and characterization of $Ru_3(CO)_7(\mu_2\text{-}H)(\mu_3\text{-}\eta^2\text{-}C{\equiv}C^tBu)$(bpcd)

The cluster $Ru_3(CO)_9(\mu_2\text{-}H)(\mu_3\text{-}\eta^2\text{-}C{\equiv}C^tBu)$ (**1**) [11] reacts with bpcd [12] in either 1,2-dichloroethane or CH_2Cl_2 with assistance from the oxidative decarbonylation reagent Me_3NO to afford the bpcd-substituted cluster $Ru_3(CO)_7(\mu_2\text{-}H)(\mu_3\text{-}\eta^2\text{-}C{\equiv}C^tBu)$(bpcd) (**2**). Cluster **2** may be isolated as an orange–brown solid in yields up to 76% by chromatography over silica gel using CH_2Cl_2 as the eluent. Eq. (1) shows the reaction under examination.

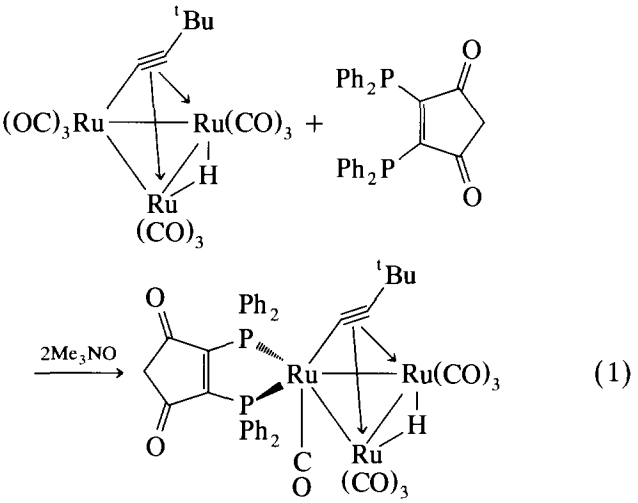

(1)

The infrared spectrum of **2** in C_6H_{12} exhibits terminal ν(CO) bands at 2064 (s), 2046 (vs), 2004 (vs), 1987 (s) and 1943 (w) cm^{-1}, while the ν(CO) bands at 1747 (w) and 1717 (m) cm^{-1} are assigned to the dione moiety associated with the bpcd ligand, on the basis of the frequency similarity to cyclopenten-3,5-dione and 4,5-dichloro-4-cyclopenten-1,3-dione [13]. The ^1H NMR spectrum of **2** displays a high-field triplet (1H) at δ −21.38 (J_{P-H} = 1.6 Hz), and is in full agreement with the existence of a bridging hydride ligand. The methylene protons of the bpcd ligand appear as a classical AB quartet centered at δ 3.52 with a $J/\Delta\nu$ value of 0.31 [14]. A single resonance at δ 1.68 and multiple resonances from δ 7.3 to 8.5 may be assigned to the t-butyl and phenyl groups, respectively. A single, sharp ^{31}P resonance at δ 80.7 in the $^{31}P\{^1H\}$ spectrum indicates

Table 1
X-ray crystallographic and data processing parameters for $Ru_3(CO)_7(\mu_2\text{-}H)(\mu_3\text{-}\eta^2\text{-}C{\equiv}C^tBu)$(bpcd)·$CH_2Cl_2$ (**2**)

Space group	Monoclinic, $P2_1/c$
Cell constants:	
a (Å)	21.190(1)
b (Å)	12.345(1)
c (Å)	17.272(1)
β (°)	95.075(5)
V, Å^3	4500.5(5)
Molecular formula	$C_{43}H_{34}Cl_2O_9P_2Ru_3$
Formula weight	1130.80
Formula units per cell (Z)	4
ρ (g cm^{-3})	1.667
Crystal size (mm^3)	0.15×0.15×0.62
Absorption coefficient (μ) (cm^{-1})	12.16
λ (radiation) (Å)	0.71073
Data collection method	ω
Collection range (°)	$2.0 \leqslant 2\theta \leqslant 44.0$
Total No. of data collected	5983
No. of independent data, $I > 3\sigma(I)$	3255
Total no. of variables	411
R	0.0399
R_w	0.0432
Weights	$[0.04F^2 + (\sigma F)^2]^{-1}$

that the bpcd ligand in **2** exists in a symmetrical environment consistent only with a chelating bpcd ligand. With the exception of some minor frequency differences, the spectroscopic data for **2** mirror the data reported for the related cluster $Ru_3(CO)_7(\mu_2\text{-}H)(\mu_3\text{-}\eta^2\text{-}C{\equiv}C^tBu)[(Z)\text{-}Ph_2PCH{=}CHPPh_2]$ [7b].

Table 2
Positional parameters for the non-hydrogen atoms of $Ru_3(CO)_7(\mu_2\text{-}H)(\mu_3\text{-}\eta^2\text{-}C{\equiv}C^tBu)$(bpcd) (**2**) with estimated standard deviations in parentheses [a]

Atom	x	y	z	B (Å²)
Ru(1)	0.75691(4)	0.14552(7)	0.20930(5)	2.42(2)
Ru(2)	0.84996(4)	0.01108(7)	0.15048(5)	3.30(2)
Ru(3)	0.85018(4)	0.23369(7)	0.11898(5)	3.28(2)
P(1)	0.7093(1)	0.2881(2)	0.2638(1)	2.57(5)
P(2)	0.7122(1)	0.0394(2)	0.2967(1)	2.60(5)
O(1)	0.6463(3)	0.1201(7)	0.0883(4)	5.1(2)
O(2)	0.9517(4)	−0.0836(8)	0.0555(5)	7.4(2)
O(3)	0.8579(4)	−0.1677(7)	0.2709(5)	6.9(2)
O(4)	0.7333(4)	−0.0941(7)	0.0653(5)	6.1(2)
O(5)	0.8565(4)	0.4641(6)	0.1828(5)	5.3(2)
O(6)	0.7372(4)	0.2897(8)	0.0062(5)	6.3(2)
O(7)	0.9540(4)	0.276(1)	0.0112(6)	9.3(3)
O(12)	0.6041(4)	0.3829(6)	0.3871(4)	4.7(2)
O(14)	0.5948(3)	0.0070(6)	0.4182(4)	3.8(2)
C(1)	0.6873(4)	0.1293(9)	0.1375(6)	3.4(2)
C(2)	0.9154(5)	−0.049(1)	0.0928(7)	4.7(3)
C(3)	0.8554(5)	−0.0997(9)	0.2268(7)	4.4(3)
C(4)	0.7751(5)	−0.0539(9)	0.0979(6)	4.2(3)
C(5)	0.8546(5)	0.3758(9)	0.1600(6)	3.8(2)
C(6)	0.7779(5)	0.269(1)	0.0516(6)	4.3(3)
C(7)	0.9173(6)	0.259(1)	0.0518(7)	5.6(3)
C(11)	0.6587(4)	0.2324(8)	0.3362(5)	2.7(2)
C(12)	0.6150(5)	0.2878(8)	0.3870(6)	3.1(2)
C(13)	0.5880(5)	0.2007(9)	0.4353(6)	3.4(2)
C(14)	0.6113(4)	0.0958(8)	0.4038(5)	2.6(2)
C(15)	0.6582(4)	0.1249(8)	0.3465(5)	2.5(2)
C(16)	0.8485(4)	0.1503(8)	0.2327(5)	2.8(2)
C(17)	0.9083(4)	0.1428(9)	0.2139(6)	3.3(2)
C(18)	0.9753(5)	0.148(1)	0.2487(7)	4.3(3)
C(19)	0.9866(6)	0.263(1)	0.2783(9)	7.2(4)
C(20)	0.9814(6)	0.071(1)	0.3177(8)	6.7(4)
C(21)	1.0233(5)	0.121(1)	0.1935(9)	7.3(4)
C(111)	0.7558(4)	0.3913(8)	0.3201(5)	2.8(2) [b]
C(112)	0.8180(5)	0.3677(9)	0.3493(6)	3.7(2) [b]
C(113)	0.8538(5)	0.445(1)	0.3903(7)	4.7(3) [b]
C(114)	0.8284(6)	0.545(1)	0.4005(7)	4.8(3) [b]
C(115)	0.7689(6)	0.569(1)	0.3739(7)	5.3(3) [b]
C(116)	0.7304(5)	0.4909(9)	0.3348(6)	3.9(2) [b]
C(117)	0.6534(4)	0.3674(8)	0.2005(6)	3.0(2) [b]
C(118)	0.6753(5)	0.4476(8)	0.1543(6)	3.3(2) [b]
C(119)	0.6323(5)	0.503(1)	0.1016(6)	4.1(2) [b]
C(120)	0.5711(5)	0.4805(9)	0.0977(6)	4.0(2) [b]
C(121)	0.5478(5)	0.4020(9)	0.1421(6)	4.1(2) [b]
C(122)	0.5898(5)	0.3437(9)	0.1937(6)	3.9(2) [b]
C(211)	0.7597(5)	−0.0189(9)	0.3799(6)	3.3(2) [b]
C(212)	0.8207(5)	0.015(1)	0.3996(7)	4.5(2) [b]
C(213)	0.8571(6)	−0.028(1)	0.4640(7)	5.5(3) [b]
C(214)	0.8328(6)	−0.104(1)	0.5073(8)	5.9(3) [b]
C(215)	0.7716(5)	−0.139(1)	0.4905(7)	5.0(3) [b]
C(216)	0.7349(5)	−0.097(1)	0.4267(7)	4.4(2) [b]
C(217)	0.6617(4)	−0.0711(8)	0.2595(6)	3.1(2) [b]
C(218)	0.5997(5)	−0.0509(9)	0.2295(6)	3.8(2) [b]
C(219)	0.5623(5)	−0.133(1)	0.1957(7)	5.1(3) [b]
C(220)	0.5870(6)	−0.235(1)	0.1913(8)	6.4(3) [b]
C(221)	0.6478(7)	−0.256(1)	0.2184(8)	6.6(3) [b]
C(222)	0.6860(5)	−0.174(1)	0.2530(7)	4.8(3) [b]
Cl(1)	0.4031(3)	0.2601(5)	0.5262(5)	15.1(2)
Cl(2)	0.4963(4)	0.3977(7)	0.5699(7)	23.5(4)
C(1s)	0.4180(9)	0.386(2)	0.536(1)	10.2(5) [b]
C(2s)	0.4525(8)	0.373(2)	0.662(1)	9.5(5) [b]

[a] Anisotropically refined atoms are given in the form of the isotropic equivalent displacement parameter defined as $(4/3)[a^2B(1,1)+b^2B(2,2)+c^2B(3,3)+ab(\cos\gamma)B(1,2)+ac(\cos\beta)B(1,3)+bc(\cos\alpha)B(2,3)]$.
[b] These atoms were refined isotropically.

2.2. X-ray diffraction structure of $Ru_3(CO)_7(\mu_2\text{-}H)(\mu_3\text{-}\eta^2\text{-}C{\equiv}C^tBu)$(bpcd)

The molecular structure of **2** was established by X-ray diffraction analysis. Cluster **2** exists as discrete molecules in the unit cell with no unusually short inter- or intramolecular contacts. The X-ray data processing and collection parameters are listed in Table 1. Tables 2 and 3 give the final fractional coordinates and selected bond distances and angles, respectively. The ORTEP diagram for **2**, which is shown in Fig. 1, reveals the chelating disposition of the bpcd ligand at the unique ruthenium center [Ru(1)] and the five-vertex polyhedral core expected for a closo trigonal bipyramid [15].

The triruthenium frame is approximated by a near equilateral triangle based on the Ru–Ru bond distances that range from 2.802(1) to 2.841(1) Å. The origin of this deviation of the metallic core from equal Ru–Ru bond lengths results from bpcd elongation of the non-hydride-bridged Ru–Ru vectors, as observed in other P-substituted triruthenium clusters of this genre [6]. Accordingly, the shorter Ru(2)–Ru(3) distance of 2.802(1) Å is assigned to the hydride-bridged Ru–Ru vector. In the case of **2**, the bridging acetylide ligand forces the μ_2-hydride below the triruthenium plane and promotes the observed shortening of the Ru(2)–Ru(3) vector [16]. The observed Ru(1)–Ru(2) and Ru(1)–Ru(3) bond elongation in **2** is presumed to result from a combination of electronic and steric effects originating from the ancillary bpcd ligand. Substitution of two strong π-accepting CO ligands by the σ-donating bpcd ligand is predicted to lead to longer Ru(1)–Ru(2) and Ru(1)–Ru(3) bonds based on the *trans* influence exerted on the cluster core by the bpcd phosphine ligand relative to the replaced CO ligands [17]. Steric repulsions between the bpcd and the bridging alkynyl ligand would also be relieved by distortion of the Ru_3 core.

The mean Ru–CO distance of 1.90 Å is within the range of those distances reported for other alkynyl-bridged Ru_3 clusters [6] and the Ru–C(σ, π) distances of the coordinated alkynyl ligand are unexceptional with respect to the parent cluster $Ru_3(CO)_9(\mu_2\text{-H})(\mu_3\text{-}\eta^2\text{-C}\equiv\text{C}^t\text{Bu})$ [3] and related P-substituted clusters [6]. No major structural perturbations within the bpcd ligand are seen as a result of coordination to the Ru(1) center. However, the planes defined by the Ru_3 core and the bpcd core oxygen and carbon atoms lead to a dihedral angle of 11.3°, tipped up from the Ru_3 plane and the normal equatorial plane.

2.3. Electrochemical studies

Cyclic voltammetric studies on cluster **2** and the free bpcd ligand were conducted at a platinum disk electrode in MeCN solvent containing 0.1 M tetra-n-butylammonium perchlorate (TBAP) as the supporting electrolyte. These data are summarized in Table 4. Cluster **2** exhibits a reversible one-electron reduction at $E_{1/2} = -0.79$ V, on the basis of peak current (I_{p^a}/I_{p^c}) ratios of unity and the linear plots of the current function (I_p) as a function of the square root of the scan rate (ν) over scan rates from 0.05 to 1.0 V s^{-1} [18]. An irreversible multi-electron oxidation wave is observed at $E_{p^a} = 0.82$ V. Increasing the scan rate to 2 V s^{-1} and dropping the temperature to −30°C did not lead to any noticeable reverse reduction wave. The room temperature cyclic voltammogram of **2** is shown in Fig. 2.

We also examined the CV behavior of the bpcd ligand because the redox data have not been reported, to our knowledge. Whereas common diphosphine ligands such as dppm and dppe do not reveal any reduction behavior down to ca. −1.5 V in MeCN solvent, the redox-active diphosphine ligands bpcd and 2,3-bis(di-

Table 3
Selected bond distances (Å) and angles (°) in $Ru_3(CO)_7(\mu_2\text{-H})(\mu_3\text{-}\eta^2\text{-C}\equiv\text{C}^t\text{Bu})$(bpcd) (**2**) [a]

Bond distances			
Ru(1)–Ru(2)	2.833(1)	Ru(1)–Ru(3)	2.841(1)
Ru(2)–Ru(3)	2.802(1)	Ru(1)–P(1)	2.274(3)
Ru(1)–P(2)	2.268(3)	Ru(1)–C(16)	1.949(9)
Ru(2)–C(16)	2.232(9)	Ru(3)–C(16)	2.220(9)
Ru(2)–C(17)	2.27(1)	Ru(3)–C(17)	2.26(1)
Ru(1)–C(1)	1.852(9)	Ru(2)–C(2)	1.93(1)
Ru(2)–C(3)	1.90(1)	Ru(2)–C(4)	1.93(1)
Ru(3)–C(5)	1.89(1)	Ru(3)–C(6)	1.89(1)
Ru(7)–C(7)	1.94(1)	P(1)–C(11)	1.850(9)
P(2)–C(15)	1.83(1)	O(1)–C(1)	1.17(1)
O(2)–C(2)	1.13(1)	O(3)–C(3)	1.13(1)
O(4)–C(4)	1.12(1)	O(5)–C(5)	1.16(1)
O(6)–C(6)	1.14(1)	O(7)–C(7)	1.11(1)
O(12)–C(12)	1.20(1)	O(14)–C(14)	1.18(1)
C(11)–C(12)	1.50(1)	C(11)–C(15)	1.34(1)
C(12)–C(13)	1.50(1)	C(13)–C(14)	1.50(1)
C(14)–C(15)	1.51(1)	C(16)–C(17)	1.34(1)
C(17)–C(18)	1.49(1)		
Bond angles			
Ru(2)–Ru(1)–Ru(3)	59.17(3)	Ru(1)–Ru(2)–Ru(3)	60.54(3)
Ru(1)–Ru(3)–Ru(2)	60.28(3)	Ru(2)–Ru(1)–P(1)	161.85(7)
Ru(2)–Ru(1)–P(2)	104.19(7)	Ru(3)–Ru(1)–P(1)	106.65(7)
Ru(3)–Ru(1)–P(2)	159.80(7)	P(1)–Ru(1)–P(2)	86.8(1)
C(1)–Ru(1)–C(16)	149.6(4)	Ru(1)–Ru(2)–C(16)	43.2(2)
Ru(1)–Ru(2)–C(17)	76.9(2)	Ru(3)–Ru(2)–C(16)	50.8(2)
Ru(3)–Ru(2)–C(17)	51.6(3)	Ru(1)–Ru(3)–C(16)	43.2(2)
Ru(1)–Ru(3)–C(17)	76.8(3)	C(16)–C(17)–C(18)	142(1)
Ru(1)–C(1)–O(1)	175.1(9)	Ru(2)–C(2)–O(2)	176(1)
Ru(2)–C(3)–O(3)	178(1)	Ru(2)–C(4)–O(4)	177(1)
Ru(3)–C(5)–O(5)	177.8(9)	Ru(3)–C(6)–O(6)	175(1)
Ru(3)–C(7)–O(7)	177(1)	P(1)–C(11)–C(12)	130.7(7)
P(1)–C(11)–C(15)	118.0(7)	C(12)–C(11)–C(15)	111.3(8)
O(12)–C(12)–C(11)	125.3(9)	O(12)–C(12)–C(13)	128(1)
C(11)–C(12)–C(13)	106.5(8)	C(12)–C(13)–C(14)	105.2(8)
O(14)–C(14)–C(13)	127.5(9)	O(14)–C(14)–C(15)	125.6(9)
C(13)–C(14)–C(15)	106.8(8)	C(11)–C(15)–C(14)	109.6(8)
P(2)–C(15)–C(11)	119.8(7)	P(2)–C(15)–C(14)	130.5(7)

[a] Numbers in parentheses are estimated standard deviations in the least significant digits.

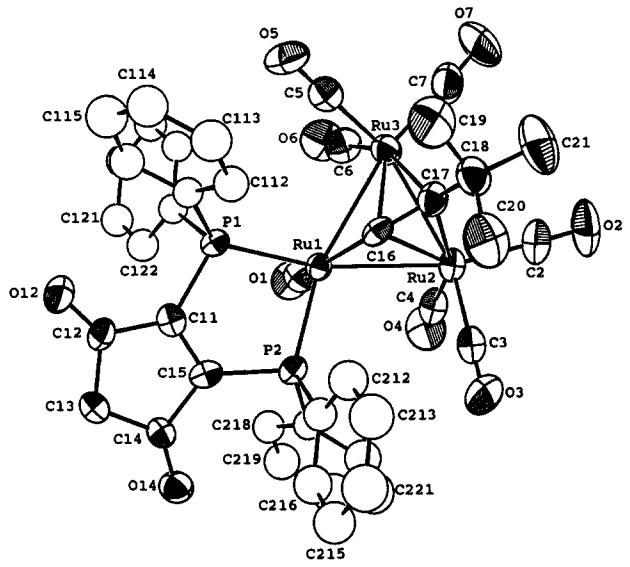

Fig. 1. ORTEP drawing of the non-hydrogen atoms of $Ru_3(CO)_7(\mu_2\text{-}H)(\mu_3\text{-}\eta^2\text{-}C{\equiv}C^tBu)(bpcd)$ (2). Thermal ellipsoids are drawn at the 50% probability level.

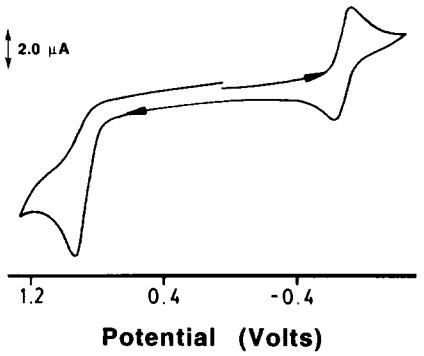

Fig. 2. Cathodic scan cyclic voltammogram of $Ru_3(CO)_7(\mu_2\text{-}H)(\mu_3\text{-}\eta^2\text{-}C{\equiv}C^tBu)(bpcd)$ (2) (ca. 10^{-3} M) in MeCN at room temperature containing 0.1 M TBAP and a scan rate of 0.1 V s^{-1}.

phenylphosphino)maleic anhydride (bma) do display accessible reduction wave(s) at lower reduction potentials owing to the presence of the electron-withdrawing 1,3-dione and maleic anhydride functionalities [19]. A quasi-reversible one-electron reduction at $E_{1/2} = -1.15$ V has been recorded for the bpcd ligand under conditions identical with those employed for cluster **2**. A current ratio of 0.74 has been measured for the $0/-1$ redox couple of this ligand at a scan rate of 0.1 V s^{-1}. The observed current deviation from unity suggests that the kinetic complications are responsible for the quasi-reversible behavior. Unlike the bma ligand, which exhibits two close one-electron reduction waves at $E_{1/2} =$ -0.63 and -1.38 V, assignable to the $0/-1$ and $-1/-2$ redox couples [8c], the bpcd ligand displays only the $0/-1$ redox couple over this potential range. The less electron-withdrawing 1,3-dione moiety manifests itself in a more negative reduction potential for the $0/-1$ redox couple in comparison with the bma ligand with its strongly electron-withdrawing maleic anhydride ligand.

Table 4
Cyclic voltammetric data for clusters **1** and **2** and bpcd [a]

Compound	Redox couple [b]					
	$0/-1$			$0/+1$		
	$E_p{}^c$	$E_p{}^a$	$E_{1/2}$	$E_p{}^a$	$E_p{}^c$	$E_{1/2}$
1 [c]	−1.93	–	–	1.23	–	–
2 [d]	−0.83	−0.75	−0.79	0.82	–	–
bpcd [e,f]	−1.10	−1.20	−1.15	1.26	–	–

[a] In ca. 10^{-3} M MeCN solutions containing 0.1 M TBAP at room temperature and a scan rate of 0.1 V s^{-1}. Potentials are in volts relative to a silver wire quasi-reference electrode, calibrated against ferrocene.
[b] $E_p{}^c$ and $E_p{}^a$ refer to the cathodic and anodic peak potentials of the CV waves. The half-wave potential $E_{1/2}$, which represents the chemically reversible redox couple, is defined as $(E_{p^c} + E_{p^a})/2$.
[c] See Ref. [20] for the initial electrochemical report on cluster **1**.
[d] A current ratio (I_{p^a}/I_{p^c}) of 1.0 was observed or the $0/-1$ redox couple.
[e] A current ratio (I_{p^a}/I_{p^c}) of 0.74 was observed for the $0/-1$ redox couple.
[f] See Ref. [30] for the polarographic reduction data for the bpcd ligand.

The effect of the coordinated bpcd ligand on cluster **2** is readily seen in the redox potential of the $0/-1$ redox couple. The one-electron reduction observed in cluster **2** is predicted to occur largely at the redox-active bpcd ligand [19]. The 0.36 V potential shift in the $0/-1$ redox couple in **2** relative to the free ligand is not surprising as the electron density associated with the bpcd ligand is diminished on coordination. We have also included the CV data for the parent cluster, recorded under identical conditions, in Table 4 for comparative purposes. The electrochemical properties of $Ru_3(CO)_9(\mu_2\text{-}H)(\mu_3\text{-}\eta_2\text{-}C{\equiv}C^tBu)$ have been reported [20]. In comparison, cluster **1** undergoes an irreversible reduction at $E_{p^c} = -1.93$ V, a more negative potential relative to that in cluster **2** with its coordinated diphosphine ligand. In the absence of a low-lying, ligand-based LUMO, the expected potential shift of the LUMO in **2** is predicted to be of the order of -0.4 V relative to the parent cluster (-0.2 V decrease per added P-ligand) [21]. This dichotomy is readily explained by the intervention of a ligand-based LUMO that serves as the site for electron accession in the $0/-1$ redox couple in cluster **2**. The redox modulation of polynuclear systems by electron-accepting ligands such as bpcd and bma promises to provide novel redox compounds with possible materials applications in solid-state devices.

2.4. Extended Hückel calculations

The composition of the HOMO and LUMO in cluster **2** was probed by carrying out extended Hückel molecular orbital calculations on the model cluster compound

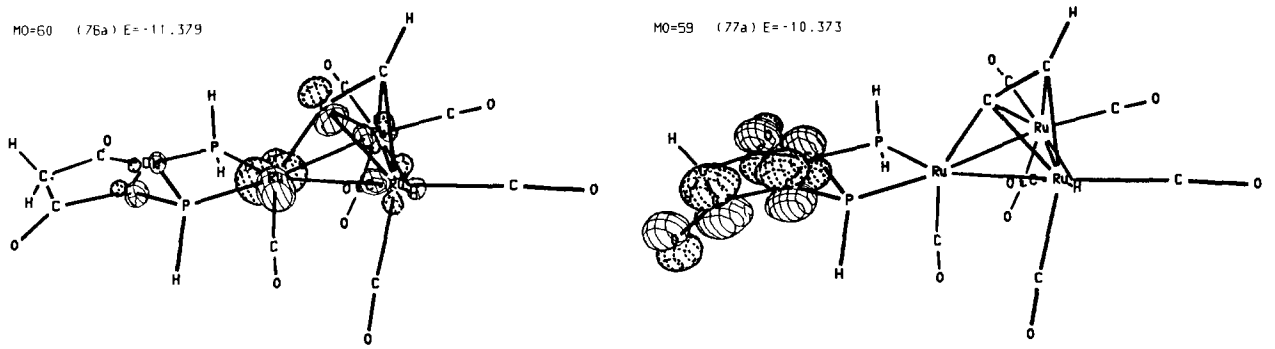

Fig. 3. CACAO drawings of the HOMO (left) and the LUMO (right) for $Ru_3(CO)_7(\mu_2\text{-}H)(\mu_3\text{-}\eta^2\text{-}C{\equiv}CH)(H_4\text{-bpcd})$.

$Ru_3(CO)_7(\mu_2\text{-}H)(\mu_3\text{-}\eta^2\text{-}C{\equiv}CH)(H_4\text{-bpcd})$. Here the t-butyl and phenyl groups were removed from the crystallographic structure of cluster **2** and were replaced by hydrogen groups. Fig. 3 shows the three-dimensional CACAO drawings of these molecular orbitals [22].

The HOMO in cluster **2** is found at -11.7 eV and is best described as a ruthenium-based orbital, with the largest contribution being the $d_{x^2-y^2}$ orbital (43%) at the bpcd-substituted Ru(1) center. The Ru(2) and Ru(3) centers bond weakly with the Ru(1). In keeping with the general MO results for other trimetal clusters, the HOMO in **2** may be considered as a Ru–Ru bonding orbital [23]. Calculations at the CNDO level on $Ru_3(CO)_9(\mu_2\text{-}H)(\mu_3\text{-}\eta^2\text{-}C{\equiv}C^tBu)$ are also in agreement with the metal-based nature of the HOMO in **2** [24].

The extended Hückel calculations indicate that the LUMO occurs at -10.4 eV and resides entirely on the bpcd ligand in a MO that is nodally similar to Ψ_4 of a six π-electron system [8c]. This π^* system is in full agreement with the electrochemical reduction data for **2**, which place the site of electron accession on the ancillary bpcd ligand. One important aspect of employing a redox-active ligand such as bpcd in the coordination sphere of a metal cluster is that the LUMO no longer consists of an antibonding array of metal framework orbitals. Electron occupation of such antibonding orbitals has been shown to lead to facile cluster fragmen-

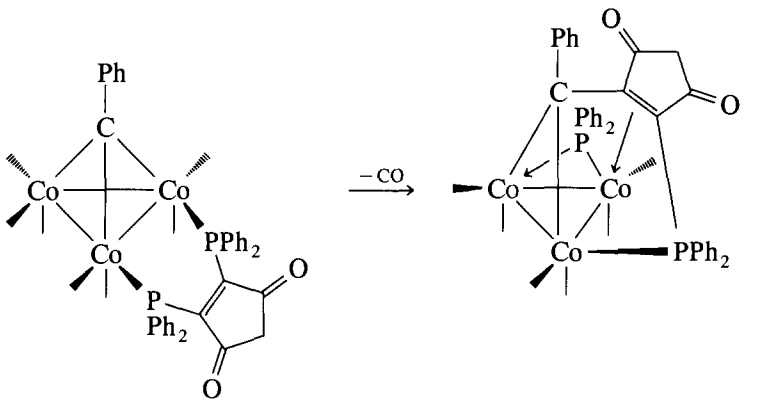

(2)

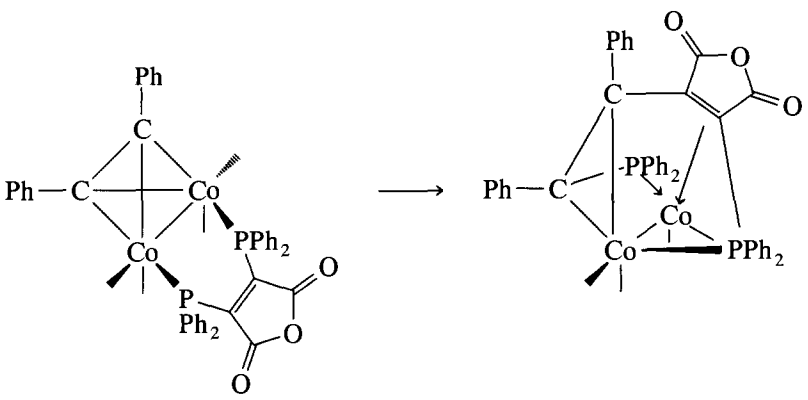

(3)

tation. Our data suggest that new and stable paramagnetic clusters can be prepared through the use of suitable redox-active diphosphine ligands.

2.5. Thermal stability of $Ru_3(CO)_7(\mu_2\text{-}H)(\mu_3\text{-}\eta^2\text{-}C{\equiv}C^tBu)(bpcd)$

The thermolysis reactivity in cluster **2** was investigated owing to our observation of facile P–C bond activation in $RCCo_3(CO)_7$(bpcd) (where R = Ph, ferrocenyl) [10a]. Similar P–C bond activation has also been reported in a bma-substituted dicobalt dimer containing a diphenylacetylene ligand [8c]. These reactions are illustrated in Eqs. (2) and (3), respectively. Therefore, it was of interest to test for analogous reactivity with the coordinated acetylide ligand in **2**. It was hoped that P–C bond cleavage would be followed by the coupling of the acetylide and dione ligands in **2**.

Unlike the above transformations, which occur readily over the temperature range 40–80°C, cluster **2** was found to be stable in refluxing toluene and *m*-xylene solutions. This stands in sharp contrast to our preliminary data on the corresponding phenylacetylide cluster $Ru_3(CO)_7(\mu_2\text{-}H)(\mu_3\text{-}\eta^2\text{-}C{\equiv}CPh)$(bpcd), which reacts in refluxing toluene to give a product displaying P–C bond cleavage [25]. The subtle effects of the acetylide R group in controlling the thermal reactivity of the ancillary bpcd ligand will be the focus our future research efforts.

3. Conclusions

The reaction between $Ru_3(CO)_9(\mu_2\text{-}H)(\mu_3\text{-}\eta^2\text{-}C{\equiv}C^tBu)$ and the redox-active bpcd ligand proceeds regioselectively to give the chelating cluster $Ru_3(CO)_7(\mu_2\text{-}H)(\mu_3\text{-}\eta^2\text{-}C{\equiv}C^tBu)$(bpcd). X-ray diffraction analysis has shown that the bpcd ligand occupies the equatorial sites at the unique ruthenium center. The electrochemical and extended Hückel MO data reveal that cluster **2** exhibits an accessible one-electron reduction, with the bpcd ligand functioning as the site for electron accession.

4. Experimental section

The starting $Ru_3(CO)_{12}$ cluster was synthesized from $RuCl_3 \cdot nH_2O$, using the carbonylation procedure of Bruce et al. [26] and $Ru_3(CO)_9(\mu_2\text{-}H)(\mu_3\text{-}\eta^2\text{-}C{\equiv}C^tBu)$ [11] and bpcd [12] were prepared by using the reported literature procedures. All halogenated solvents were distilled from P_2O_5 under argon using Schlenk techniques [27]. Toluene and MeCN were distilled from sodium–benzophenone and CaH_2, respectively. All purified solvents were stored in Schlenk storage vessels equipped with Teflon stopcocks. The TBAP used in the CV studies was obtained from Johnson Matthey Electronics and was recrystallized from ethyl acetate–light petroleum, followed by drying for 2 days under vacuum. C and H microanalyses were performed by Atlantic Microlab (Norcross, GA, USA).

Infrared spectra were recorded on a Nicolet 20 SXB FT-IR spectrometer in 0.1 mm NaCl cells. ^1H and ^{31}P NMR spectra were recorded in $CDCl_3$ solvent at 200 and 121 MHz on a Varian Gemini-200 spectrometer and a Varian VXR-300 spectrometer, respectively. The reported ^{31}P chemical shift was referenced to external H_3PO_4 (85%), with the positive chemical shift to low field of the external standard.

4.1. Synthesis of $Ru_3(CO)_7(\mu_2\text{-}H)(\mu_3\text{-}\eta^2\text{-}C{\equiv}C^tBu)$(bpcd)

To 0.25 g (0.38 mmol) of $Ru_3(CO)_9(\mu_2\text{-}H)(\mu_3\text{-}\eta^2\text{-}C{\equiv}C^tBu)$ and 0.19 g (0.40 mmol) bpcd in a Schlenk tube were added 50 ml of CH_2Cl_2, followed by 61.8 mg (0.82 mmol) of Me_3NO. The reaction solution was stirred overnight under argon and then examined by IR and TLC analyses. After solvent removal under vacuum, the product was isolated by chromatography over silica gel using CH_2Cl_2 as the eluent. The analytical sample and single crystals of **2** suitable for X-ray analysis were grown from a CH_2Cl_2 solution containing **2** that had been layered with pentane; yield 0.31 g (76%). IR (CH_2Cl_2): ν(CO) 2064 (s), 2046 (vs), 2004 (vs), 1987 (s), 1943 (w), 1747 (w, bpcd) and 1717 (m, bpcd) cm^{-1}. ^1H NMR ($CDCl_3$): δ −21.38 (1H, t, J_{P-H} = 1.6 Hz), 1.68 (9H, s, ^tBu), 3.52 (2H, AB quartet, J = 21.6 Hz), aromatic multiplet 7.3 to 8.5 (20H). $^{31}P\{^1H\}$ NMR spectrum ($CDCl_3$): δ 80.7. Anal. Found: C, 45.68; H, 3.00. Calc. for $C_{42}H_{33}O_9P_2Ru_3 \cdot CH_2Cl_2$: C, 45.67; H, 3.08%.

4.2. X-ray diffraction structure of $Ru_3(CO)_7(\mu_2\text{-}H)(\mu_3\text{-}\eta^2\text{-}C{\equiv}C^tBu)$(bpcd)

An orange–brown crystal of dimensions 0.15 × 0.15 × 0.62 mm was sealed inside a Lindemann capillary and then mounted on the goniometer of an Enraf-Nonius CAD-4 diffractometer. The radiation used was Mo Kα monochromatized by a crystal of graphite. Cell constants were obtained from a least-squares refinement of 25 reflections with $2\theta > 30°$. Intensity data in the range $2.0 \geqslant 2\theta \geqslant 44°$ were collected at room temperature using the ω-scan technique in the variable-scan speed mode and were corrected for Lorentz, polarization and absorption (DIFABS). Three reflections (1000, 080, 0010) were measured after every 3600 s of exposure time as a check of crystal stability (< 3%). The structure was solved by using a Patterson map, and all of the non-hydrogen atoms were located with difference Fourier maps and refined by using full-matrix

least-squares methods. The bridging hydride that spans the Ru(2)–Ru(3) bond was not located satisfactorily and was not included. Other H atoms were included in the model at idealized positions (dC–H = 0.95 Å). With the exception of the phenyl and solvent carbon atoms, all non-hydrogen atoms were refined anisotropically. Refinement converged at $R = 0.0399$ and $R_w = 0.0432$ for 3255 unique reflections with $I > 3\sigma(I)$.

4.3. Electrochemical studies

Cyclic voltammetric experiments were carried out by using a PAR Model 273 potentiostat/galvanostat, equipped with positive feedback circuitry in order to compensate for *IR* drop. The three-electrode cell used in the CV studies was of laboratory-made design, allowing for all cyclic voltammograms to be obtained under oxygen- and moisture-free conditions. All CV experiments employed a platinum disk (area = 0.0079 cm^2) as the working and auxiliary electrode. All voltammograms utilized a silver wire quasi-reference electrode, with the quoted potential data being referenced to the formal potential of the Cp_2Fe/Cp_2Fe^+ (internally added) redox couple, taken to have $E_{1/2} = 0.307$ V [18].

4.4. Molecular orbital calculations

The extended Hückel calculations reported here were carried out with the original program developed by Hoffmann and Lipscomb [28], as modified by Mealli and Proserpio [22]. The input Z-matrix for $Ru_3(CO)_7(\mu_2\text{-H})(\mu_3\text{-}\eta^2\text{-C}{\equiv}\text{CH})(H_4 - \text{bpcd})$ was constructed by replacing the phenyl groups on the bpcd ligand and the t-butyl group on the acetylide ligand with hydrogen groups using the PC modeling program MOBY. The C–H (1.06 Å) and P–H (1.42 Å) distances used in the extended Hückel calculations were taken from model compounds [29].

Acknowledgments

We thank Professor Carlo Mealli for providing us with a copy of his CACAO drawing program. Financial support from the Robert A. Welch Foundation (B-1202-SGB and B-1039-MGR) and the UNT Faculty Research Program is gratefully appreciated.

References and notes

[1] (a) G. Lavigne, in D.F. Shriver, H.D. Kaesz and R.D. Adams (eds.), *The Chemistry of Metal Cluster Complexes*, VCH, New York, 1990, Chapter 5; (b) A.J. Deeming, in B.F.G. Johnson (ed.), *Transition Metal Clusters*, Wiley, New York, 1980, Chapter 6; (c) B.C. Gates, L. Guczi, and H. Knözinger (eds.), *Metal Clusters in Catalysis*, Elsevier, New York, 1986; (d) P.R. Raithby and M.J. Rosales, *Adv. Inorg. Chem. Radiochem.*, *29* (1985) 169; (e) E. Sappa, A. Tiripicchio and P. Braunstein, *Chem. Rev.*, *83* (1983) 203; (f) R.D. Adams, *Chem. Soc. Rev.*, (1994) 335.

[2] E. Sappa, O. Gambino, L. Milone and G. Centini, *J. Organomet. Chem.*, *39* (1972) 169.

[3] M. Catti, G. Gervasio and S.A. Mason, *J. Chem. Soc., Dalton Trans.*, (1977) 2260.

[4] For the structure and chemistry of related alkynyl-bridged clusters, see: (a) P. Braunstein, G. Predieri, A. Tiripicchio and E. Sappa, *Inorg. Chim. Acta*, *63* (1982) 113; (b) E. Sappa, A.M.M. Lanfredi and A. Tiripicchio, *Inorg. Chim. Acta*, *36* (1978) 197; (c) R. Fahmy, K. King, E. Rosenberg, A. Tiripicchio and M.T. Camellini, *J. Am. Chem. Soc.*, *102* (1980) 3626; (d) C. Barner-Thorsen, E. Rosenberg, G. Saatjian, S. Aime, L. Milone and D. Osella, *Inorg. Chem.*, *20* (1981) 1592, (e) S. Aime, G. Gervasio, L. Milone, E. Sappa, and M. Franchini-Angela, *Inorg. Chim. Acta*, *26* (1978) 223; (f) E. Rosenberg, E.V. Anslyn, C. Barner-Thorsen, S. Aime, D. Osella, R. Gobetto and L. Milone, *Organometallics*, *3* (1984) 1790; (g) G. Gervasio, E. Sappa, A.M.M. Lanfredi and A. Tiripicchio, *Inorg. Chim. Acta*, *68* (1983) 171; (h) E. Rosenberg, J. Wang and R.W. Gellert, *Organometallics*, *7* (1988) 1093; (i) S. Hajela, B.M. Novak, and E. Rosenberg, *Organometallics*, *8* (1989) 468; (j) C. Barner-Thorsen, K.I. Hardcastle, E. Rosenberg, J. Siegel, A.M.M. Lanfredi, A. Tiripicchio and M.T. Camellini, *Inorg. Chem.*, *20* (1981) 4306.

[5] (a) P. Ewing and L.J. Farrugia, *Organometallics*, *8* (1989) 1246; (b) L.J. Farrugia, *Organometallics*, *9* (1990) 105; (c) E. Sappa, A. Tiripicchio and M.T. Camellini, *Inorg. Chim. Acta*, *41* (1980) 11; (d) E. Sappa, A.M.M. Lanfredi and A. Tiripicchio, *J. Organomet. Chem.*, *221* (1981) 93.

[6] (a) A.J. Carty, S.A. MacLaughlin, N.J. Taylor and E. Sappa, *Inorg. Chem.*, *20* (1981) 4437; (b) E. Sappa, G. Pasquinelli, A. Tiripicchio and M.T. Camellini, *J. Chem. Soc., Dalton Trans.*, (1989) 601; (c) C. Jangala, E. Rosenberg, D. Skinner, S. Aime, L. Milone and E. Sappa, *Inorg. Chem.*, *19* (1980) 1571; (d) E. Sappa, *J. Organomet. Chem.*, *352* (1988) 327; (e) L.J. Farrugia and S.E. Rae, *Organometallics*, *11* (1992) 196.

[7] (a) G. Predieri, A. Tiripicchio, C. Vignali and E. Sappa, *J. Organomet. Chem.*, *342* (1988) C33; (b) E. Sappa, G. Predieri, A. Tiripicchio and C. Vignali, *J. Organomet. Chem.*, *378* (1989) 109.

[8] (a) W.H. Watson, A. Nagl, S. Hwang and M.G. Richmond, *J. Organomet. Chem.*, *445* (1993) 163; (b) K. Yang, J.M. Smith, S.G. Bott and M.G. Richmond, *Organometallics*, *12* (1993) 4779; (c) K. Yang, S.G. Bott and M.G. Richmond, *Organometallics*, *13* (1994) 3788; (d) K. Yang, S.G. Bott and M.G. Richmond, *Organometallics*, *13* (1994) 3767.

[9] C.-G. Xia, S.G. Bott and M.G. Richmond, *Inorg. Chim. Acta*, *230* (1995) 45.

[10] (a) H. Shen, S.G. Bott and M.G. Richmond, unpublished results; (b) see Refs. [8b] and [8c] for related P–C bond reactivity.

[11] E. Rosenberg and B. Novak, *Inorg. Synth.*, *26* (1989) 328.

[12] (a) D. Fenske and H.J. Becher, *Chem. Ber.*, *108* (1975) 2115; (b) D. Fenske, *Chem. Ber.*, *112* (1979) 363.

[13] D. Dolphin and A. Wick, *Tabulation of Infrared Spectral Data*, Wiley-Interscience, New York, 1977.

[14] F.A. Bovey, *Nuclear Magnetic Resonance Spectroscopy*, Academic Press, New York, 1969.

[15] For applications of polyhedral skeletal electron pair (PSEP) topology in cluster descriptions, see: (a) D.M.P. Mingos, *Nature Phys. Sci.*, *236* (1972) 99; (b) K. Wade, *Adv. Inorg. Chem. Radiochem.*, *18* (1976) 1.

[16] For a discussion on the lengthening of M–M bonds that are bridged by a hydride ligand, see: D.M.P. Mingos and D.J. Wales, *Introduction to Cluster Chemistry*, Prentice Hall, Englewood Cliffs, NJ, 1990.
[17] J.P. Collman, L.S. Hegedus, J.R. Norton and R.G. Finke, *Principles and Applications of Organotransition Metal Chemistry*, University Science Books, Mill Valley, CA, 1987, pp. 242–243.
[18] (a) A.J. Bard and L.R. Faulkner, *Electrochemical Methods*, Wiley, New York, 1980; (b) P.H. Rieger, *Electrochemistry*, Chapman and Hall, New York, 1994.
[19] For electrochemical studies involving the redox-active bma ligand, see: (a) Ref. [8c]; (b) F. Mao, D.R. Tyler and D. Keszler, *J. Am. Chem. Soc.*, *111* (1989) 130, (c) F. Mao, C.E. Philbin, T.J.R. Weakley and D.R. Tyler, *Organometallics*, *9* (1990) 1510.
[20] P. Zanello, S. Aime and D. Osella, *Organometallics*, *3* (1984) 1374.
[21] M.G. Richmond and J.K. Kochi, *Inorg. Chem.*, *25* (1986) 656, and references cited therein.
[22] C. Mealli and D.M. Proserpio, *J. Chem. Educ.*, *67* (1990) 399.
[23] (a) M.C. Manning and W.C. Trogler, *Coord. Chem. Rev.*, *38* (1981) 89; (b) B.E.R. Schilling and R. Hoffmann, *J. Am. Chem. Soc.*, *101* (1979) 3456; (c) J.C. Green, D.M.P. Mingos and E.A. Seddon, *Inorg. Chem.*, *20* (1981) 2595.
[24] G. Granozzi, E. Tondello, R. Bertoncello, S. Aime and D. Osella, *Inorg. Chem.*, *22* (1983) 744.
[25] H. Shen, S.G. Bott and M.G. Richmond, in preparation.
[26] M.I. Bruce, C.M. Jensen and N.L. Jones, *Inorg. Synth.*, *26* (1989) 259.
[27] D.F. Shriver, *The Manipulation of Air-Sensitive Compounds*, McGraw-Hill, New York, 1969.
[28] (a) R. Hoffmann and W.N. Lipscomb, *J. Chem. Phys.*, *36* (1962) 3179; (b) R. Hoffmann, *J. Chem. Phys.*, *39* (1963) 1397.
[29] R.C. Weast (ed.), *Handbook of Chemistry and Physics*, CRC Press, Cleveland, OH, 56th edn., 1975.
[30] H.J. von Becher, D. Fenske and M. Heymann, *Z. Anorg. Allg. Chem.*, *475* (1981) 27.